ELSEVIER

Journal of Nuclear Materials 277 (2000) 199–203

journal of nuclear materials

www.elsevier.nl/locate/jnucmat

Radiation damage in neutron-irradiated yttria-stabilized-zirconia single crystals

B. Savoini*, D. Cáceres, I. Vergara, R. González, J.E. Muñoz Santiuste

Departamento de Física, Escuela Politécnica Superior, Universidad Carlos III, Avda. de la Universidad 30, 28911 Leganés, Madrid, Spain

Received 19 May 1999; accepted 23 July 1999

Abstract

Optical absorption measurements and luminescence experiments have been made in neutron-irradiated or thermochemically reduced yttria-stabilized-zirconia (YSZ) crystals. Two absorption bands centered at about 375 and 470 nm were observed after irradiation or reduction; however, the thermal stability of these bands in each case is very different. In irradiated crystals the bands disappear with heat treatments at ~600 K, whereas in reduced crystals they anneal out at ~1300 K. This difference is probably due to interstitial–vacancy recombination in the oxygen sublattice of the former crystals. Nano-indentation tests show that hardness and the elastic modulus remain practically unchanged after TCR or neutron-irradiation. These results confirm that YSZ single crystals are radiation resistant and that the radiation damage can be easily removed by anneals in air at temperatures above 600 K.

1. Introduction

Yttria-stabilized zirconia (YSZ) is a solid ionic conductor with applications ranging from oxygen sensors to solid fuel cells [1]. Its high ionic conductivity at high temperatures is related to oxygen vacancies already present in the YSZ crystal associated with the charge compensation induced when Y_2O_3 is added to ZrO_2 to stabilize the cubic phase. The oxygen vacancy allocation has been extensively investigated in recent years [2–4]. This material is a candidate inert-matrix, nuclear fuel-form for the destruction of excess plutonium [5–10]. Both cubic UO_2 and PuO_2 are isostructural with cubic-zirconia. In addition, actinides are soluble in zirconia. These properties make this refractory ceramic a good candidate actinide host material for nuclear waste storage [9]. As a fuel material, the YSZ will be the host phase of Pu, U, other actinide elements or high energy fission products, and will consequently experience neutron bombardment damage. For its application in fission and fusion reactors, zirconia must retain its structural integrity under neutron-irradiation.

The behavior of zirconia-based ceramics under irradiation is not well known. Early studies showed that natural monoclinic ZrO_2 is transformed into the cubic phase under the action of fission fragments produced by fast-neutron-irradiation of impurities present in the crystal, such as uranium and thorium [11,12]. However, more recent studies in cubic-stabilized zirconia showed that this material is radiation resistant when neutron or ion irradiated and thus favor its selection as an advanced nuclear fuel for Pu incineration [9,10,13–16].

In general, defects in the form of anion vacancies can be produced in ceramic oxides by irradiation with energetic particles, such as neutrons, electrons, and ions. Elastic collisions with energetic particles do not produce cation vacancies because the cation interstitials are unstable and quickly recombine with the vacancies. In the present work, the damage introduced in single crystals of YSZ by irradiation with fast neutrons has been primarily characterized by optical measurements. Nano-indentation experiments were made to study the possible influence of the radiation damage on the mechanical properties. The results are compared with those for samples thermochemically reduced at high temperatures.

* Corresponding author. Fax: +34-91 624 9430.
E-mail address: bsavoi@fis.uc3m.es (B. Savoini).

0022-3115/00/$ - see front matter
PII: S0022-3115(99)00200-7

2. Experimental procedures

Single crystals of ZrO_2 stabilized with 16 wt% of Y_2O_3 were purchased from CERES Corporation (USA). Excellent optical quality crystals were grown by the skull method. Samples were cut with a diamond saw and polished to optical quality. Powder X-ray diffraction patterns of the samples were recorded with an X'Pert-MHD Philips diffractometer using Cu K_α radiation.

Neutron-irradiations were performed at the High Flux Reactor of the Institute for Advanced Materials of the Joint Research Center (JRC) at Petten, using fluxes of 0.78×10^{18} fission spectrum neutrons/m^2 s ($E>0.1$ MeV). The neutron doses were 1.2×10^{21} and 1.0×10^{22} neutrons/m^2, respectively. The ambient temperature was 330 K. Thermochemical reduction (TCR) was made by placing the samples inside a graphite container surrounded by flowing oxygen-free nitrogen gas inserted in a horizontal furnace.

Optical absorption measurements in the UV-VIS-IR were made with a Perkin–Elmer Lambda 19 spectrophotometer. For the luminescence experiments, the samples were excited with an ORIEL Hg(Xe) 400 W lamp. The emitted light was focused onto the entrance slit of a SPEX 1000M monochromator and detected with a Hamamatsu R943-02 cooled photomultiplier tube. The spectra were recorded with a SR400 gated photocounter.

Nano-indentation experiments were made with a Nano Indenter II s to determine the Young's modulus (E) and the hardness (H) by the Oliver and Pharr method [17]. A fused silica sample was used as a control and tested at the outset of each experiment. In each indentation experiment, the indenter was first loaded and unloaded three times in succession at a constant rate of 10% of the maximum depth and for three different depths. Each of the unloadings terminated at 10% of the peak load to assure that the contact was maintained between the specimen and the indenter. Three hold periods of 50 s were inserted at the maximum depths and another hold period of 100 s was inserted at the minimum of the final unloading. During this last hold period the displacement of the indenter was carefully monitored to establish the rate of thermal drift in the machine for subsequent correction of the data. Three experiments were carried out for maximum depths of first, 200, 250 and 300 nm; second, 400, 550 and 700 nm; and third, 900, 1200 and 1400 nm, respectively. Thus, for each sample, nine peak loads were investigated.

3. Results and discussion

X-ray analysis shows that these crystals have a well-crystallized cubic fluorite structure with a lattice parameter of 0.5146 nm, in agreement with previously reported values [18]. No change in the lattice parameter has been observed in the samples after either n-irradiation or TCR.

Undoped YSZ crystals are transparent in the as-grown state. After either neutron-irradiation or thermochemical reduction they become colored. The absorption spectra of two n-irradiated crystals with a dose of 1.2×10^{21} and 1.0×10^{22} neutrons/m^2, respectively, are shown in Fig. 1. For the sake of comparison, the absorption spectrum of a crystal thermochemically reduced for 20 min at 1273 K is also displayed. In all the spectra, a broad absorption band centered at about 470 nm is observed. The intensity of this band increases with the irradiation dose. In addition, the absorption edge shifts towards lower wavelengths in the TCR sample as previously described [19,20]. This effect was not found in n-irradiated samples. The 470 nm band has been previously associated with electrons trapped at oxygen vacancies nearest to Zr cations, and with oxygen ions with trapped holes adjacent to yttria cations [19]. The differential spectra between either the n-irradiated samples or the TCR sample and the as-grown sample reveal the presence of a shoulder at about 375 nm (Fig. 2), which has been tentatively assigned to both electrons trapped at oxygen vacancies nearest to Zr cations and to Ti^{3+} impurities [19].

The formation of the 470 nm band in TCR crystals was investigated by reducing a YSZ sample for 15 min intervals at increasing temperatures. The optical densities versus temperatures are plotted in Fig. 3. A threshold temperature for the band formation was estimated to be 1200 K.

With 16% in weight yttria, fluorite structure, lattice parameter $a=0.5146$ nm, one can calculate from the structure a theoretical density of 5900 kg/m^3,

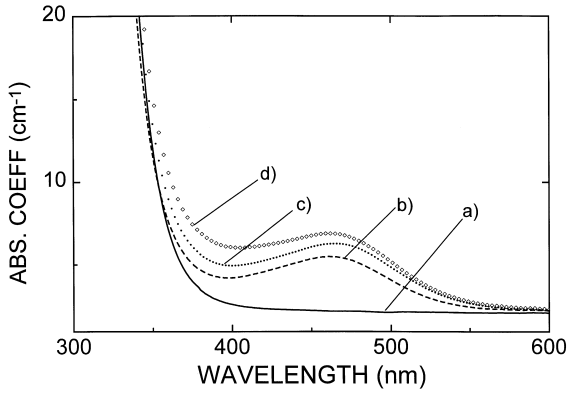

Fig. 1. Optical absorption spectra of (a) as-grown crystal, after (b) TCR at 1273 K, (c) irradiation with 1.2×10^{21} n/m^2 and (d) irradiation with 1.0×10^{22} n/m^2.

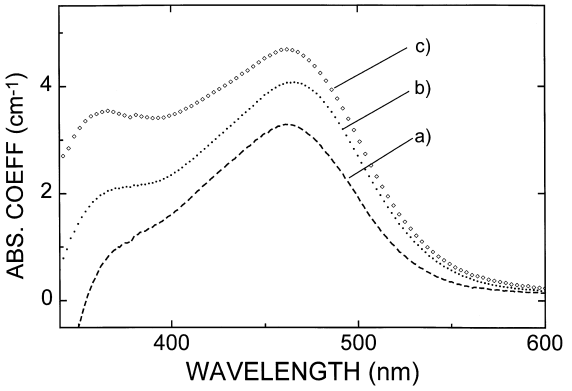

Fig. 2. Differential spectra between an as-grown sample and samples after (a) TCR at 1273 K, (b) irradiation with 1.2×10^{21} n/m^2, and (c) irradiation with 1.0×10^{22} n/m^2.

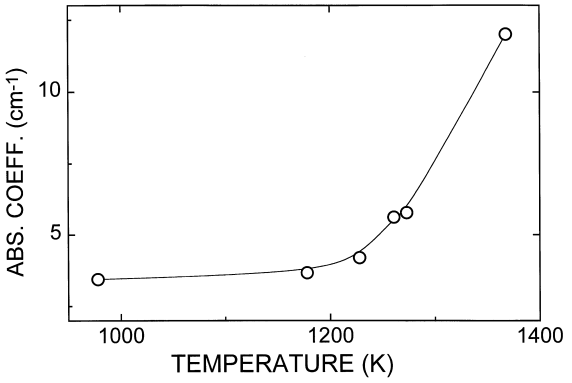

Fig. 3. Optical density versus temperature after isochronal anneals in a reducing atmosphere.

corresponding with a concentration of oxygen vacancies of $\approx3\times10^{27}$ m^{-3}. Application of the Ivey–Mollwo relation [21,22] as modified by Turner [23], to 16% in weight yttria in zirconia, yields the position of the F^+ center (an oxygen vacancy with one electron) at $6.4a^{2.4}\approx325$ nm [24], below the absorption edge. In order to determine whether n-irradiation has produced defects whose absorptions occur at wavelengths below the absorption edge and thus are undetectable by optical absorption measurements, luminescence experiments were performed at several selected wavelengths: 300, 325 and 350 nm. Also luminescence experiments were made by excitation in the peak position of the 375 and 470 nm bands. No luminescence in the visible region was observed under excitation in the latter band. Fig. 4 shows the luminescence spectrum under excitation with 325 nm light for the as-grown sample. A broad emission band centered at about 570 nm was observed, in agreement with previous findings [25–27]. In TCR and n-irradiated

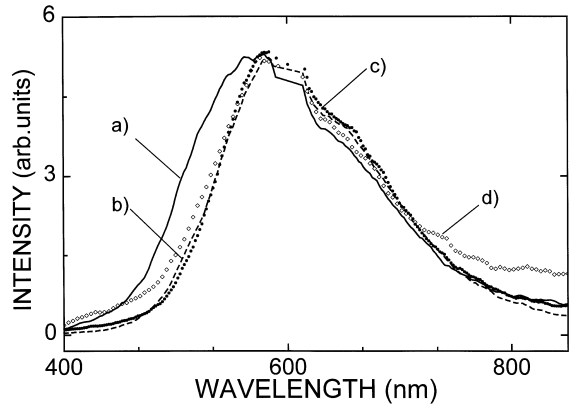

Fig. 4. Luminescence spectra under excitation with 325 nm light for (a) as-grown crystal, and after (b) TCR at 1373 K, (c) irradiated with 1.2×10^{21} n/m^2, and (d) irradiated with 1.0×10^{22} n/m^2. All the spectra were normalized at 580 nm.

samples, the peak of the emission spectra appears to be shifted to 585 nm, due to self-absorption in the lower wavelength side from the 470 nm absorption band (Fig. 2). Similar spectra were obtained when the samples were excited with 300, 350 and 375 nm.

These results indicate that most likely the band at 470 nm is associated with the same type of defects in both TCR and n-irradiated samples. This is also true for the 375 nm band. Furthermore, neither n-irradiation nor TCR appears to create new defects that are optically active below the absorption edge.

The thermal stability of the defects produced by either TCR or neutron-irradiation was studied by subjecting the samples to isochronal thermal annealings for 10 min. at increasing temperatures in air. The evolution of the intensity of the optical-absorption band at 470 nm, measured at RT, with the annealing temperature is plotted in Fig. 5. Clearly, the band of the n-irradiated crystal is much less stable than that of the TCR sample. The same is true for the shoulder at 375 nm. After thermal treatment at ~590 K, the n-irradiated bands have completely annealed out, while the bands in the TCR crystal remain stable until 1100 K and only disappear after the annealing at 1300 K. Similar results were obtained in other oxides [28,29] and this difference in stability was attributed to interstitial-vacancy recombination in the oxygen sublattice of the irradiated crystals, where the oxygen interstitials are delocalized at temperatures not much higher than RT. In TCR crystals anion vacancies can readily survive 1100 K because there are no interstitials.

Nano-indentation experiments were made to determine the effects of both n-irradiation and TCR on the mechanical properties. Fig. 6 shows a selected load–displacement curve for the as-grown sample. The shape

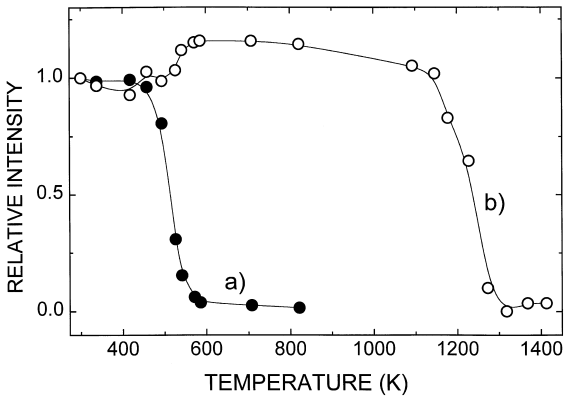

Fig. 5. Normalized intensity of the 470 nm bands versus isochronal annealing temperature of samples (a) irradiated with 1.2×10^{21} n/m^2 and (b) thermochemically reduced at 1373 K.

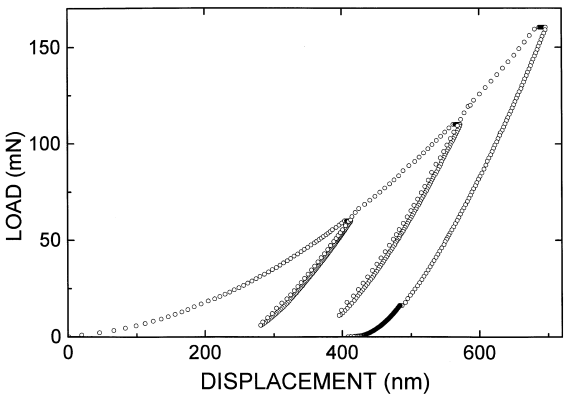

Fig. 6. Selected load–displacement curve for as-grown YSZ crystals.

of the curve is typical of most ceramics, that is, a large elastic component due to the recovery of the surface flexure coupled with a small additional recovery of the indentation depth itself [30]. Similar curves were obtained for both the TCR and the n-irradiated samples. From these load–displacement curves, and knowing the exact geometry of the indenter tip, it is possible to determine the hardness, H, and elastic modulus, E, as a function of the indenter displacement.

Fig. 7 shows the results obtained for the four types of samples tested. Data points represent the mean values of the hardness and elastic modulus at specific indentation depths, based on ten separate load–displacement tests. The standard deviation in the mean values of H (not shown in Fig. 7) divided by the mean value of H ranges from 4% at an indentation depth of 100 nm to 2% at an indentation depth of 1200 nm. The standard deviation in the mean values of E divided by the mean value of E

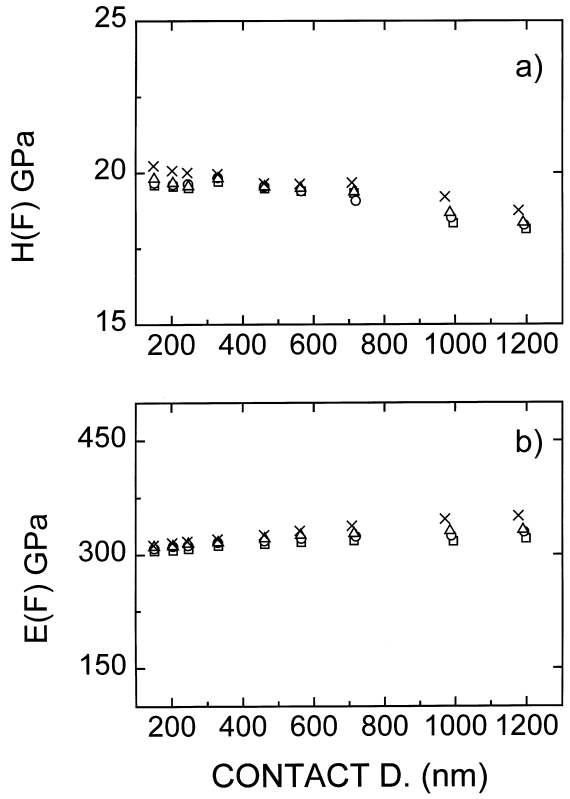

Fig. 7. (a) Hardness and (b) elastic modulus versus contact depth for as-grown crystals (□), after TCR (○), irradiated with a dose of 1.2×10^{21} n/m^2 (Δ), and 1.0×10^{22} n/m^2 (×).

ranges from 3% at an indentation depth of 100 nm to 1% at an indentation depth of 1200 nm.

The H values in Fig. 7(a) are practically independent of depth and of the treatment (TCR or n-irradiation) given to the samples. The resulting values range from 18.5 to 20 GPa, as the indentation depth varies from 100 to 1200 nm. The E values in Fig. 7(b) for the as-grown sample range between 305 and 320 GPa, in good agreement with previous findings [9]. No significant changes were observed after the samples were TCR or n-irradiated, indicating that the defects induced by either TCR or n-irradiation do not significantly change the mechanical properties of YSZ. In n-irradiated crystals, radiation hardening is expected and is caused primarily by the presence of interstitials [31,32]. The lack of hardening in our irradiated samples may be due to the fact that the concentration of interstitials is too low to produce any significant increase in hardness. Indeed, in YSZ crystals irradiated with I^+ ions, where a high concentration of interstitials should in principle be created, softening (a decrease in the elastic modulus and hardness) was observed and tentatively attributed to partial amorphization [9].

4. Summary and conclusions

Single crystals of YSZ have been neutron irradiated up to doses of 1.2×10^{21} and 1.0×10^{22} neutrons/m^2, respectively. Optical absorption measurements and luminescence experiments indicate that the optically active defects induced by irradiation are those responsible for the absorption bands at 375 and 470 nm, which have been related to charged oxygen vacancies and to oxygen ions with trapped holes [19]. These absorption bands have also been observed in YSZ crystals after TCR at temperatures higher than 1200 K. However, the bands in n irrudiated crystals are thermally much less stable than in TCR crystals. The former anneal out at ~590 K while the latter disappear only after an annealing at ~1300 K. This difference in stability is probably due to interstitial-vacancy recombination in the oxygen sublattice of the irradiated crystals. In TCR crystals anion vacancies are more stable because there are no interstitials.

Hardness and the elastic modulus of YSZ crystals were determined by Nano-indentation experiments. The resulting values were ~20 and ~305 GPa, respectively. No significant changes are induced by TCR or neutron-irradiation.

In conclusion, these results confirm that YSZ crystals are radiation resistant when irradiated with neutrons. The induced damage does not significantly change their mechanical properties. The radiation damage can easily be recovered by thermal anneals in air at temperatures above 600 K.

Acknowledgements

We are indebted to A.I. Popov for helpful discussions. This work has been supported by the Comisión Asesora de Investigación Científica y Técnica of the Spanish Government. The irradiation was carried out at the High Flux Reactor of the Institute for Advanced Materials of the JRC at Petten under contract no. 40.00024 with the European Atomic Energy Commission.

References

[1] A.H. Heure, L.W. Hobbs (Eds.), Science and Technology of Zirconia, Ser. Adv. Ceramics, vol. 3, American Ceramic Society, Columbus, OH, 1981.
[2] J. Dexper-Ghys, M. Faucher, P. Caro, J. Solid State Chem. 54 (1984) 179.
[3] M.H. Tuilier, J. Dexper-Ghys, H. Dexpert, P. Lagarde, J. Solid State Chem. 69 (1987) 153.
[4] Ping Li, I- Wei Chen, J.E. Penner-Hahn, Phys. Rev. B 48 (1993) 10074.
[5] H. Akie, T. Muromura, H. Takano, S. Matsura, Nucl. Technol. 107 (1994) 182.
[6] C. Degueldre, U. Kasemeyer, F. Botta, G. Lederberger, Mater. Res. Soc. Symp. Pro. 412 (1996) 15.
[7] C. Degueldre, P. Heimgartner, G. Ledergerber, N. Sasajima, K. Hojou, T. Muromura, L. Wang, W. Gong, R. Ewing, Mater. Res. Soc. Symp. Proc. 439 (1997) 625.
[8] N. Sasajima, T. Matsui, K. Hojou, S. Furuno, H. Otsu, K. Izui, T. Muromura, Nucl. Instrum. and Meth. B 141 (1998) 487.
[9] K.E. Sickafus, H. Matzke, K. Yasuda, P. Chodak III, R.A. Verrall, P.G. Lucuta, H.R. Andrews, A. Turos, R. Fromknecht, N.P. Baker, Nucl. Instrum. and Meth. B 141 (1998) 358.
[10] C. Degueldre, J.M. Paratte, Nucl. Technol. 123 (1998) 21.
[11] M.C. Wittels, F.A. Sherrill, J. Appl. Phys. 27 (1956) 643.
[12] M.C. Wittels, F.A. Sherrill, Phys. Rev. Lett. 3 (1959) 176.
[13] F.W. Clinard Jr., D.L. Rohr, W.A. Ranken, J. Am. Ceram. Soc. 60 (1977) 287.
[14] E.L. Fleischer, M.G. Norton, M.A. Zaleski, W. Hertl, C.B. Carter, J.W. Mayer, J. Mater. Res. 6 (1991) 1905.
[15] N. Yu, K.E. Sickafus, P. Kodali, M. Nastasi, J. Nucl. Mater. 244 (1997) 266.
[16] K. Yasuda, M. Nastasi, K.E. Sickafus, C.J. Maggiore, N. Yu, Nucl. Instrum. and Meth. B 136–138 (1998) 499.
[17] W.C. Oliver, G.M. Pharr, J. Mater. Res. 7 (1992) 1564.
[18] T.H. Etsell, S.N. Flengas, Chem. Rev. 70 (1970) 339.
[19] V.M. Orera, R.I. Merino, Y. Chen, R. Cases, P.J. Alonso, Phys. Rev. B 42 (1990) 9782.
[20] B. Savoini, C. Ballesteros, J.E. Muñoz Santiuste, R. González, Phys. Rev. B 57 (1998) 13439.
[21] E. Mollwo, Nach. Gess. Wissen, Göttingen, 1931, p. 97.
[22] H. Ivey, Phys. Rev. 72 (1947) 341.
[23] T.J. Turner, Solid State Commun. 7 (1969) 635.
[24] D.A. Wright, J.S. Thorp, A. Aypar, H.P. Buckley, J. Mater. Sci. 8 (1973) 876.
[25] M. Kunz, H. Kretschmann, W. Assmus, C. Klingshirn, J. Lumin. 37 (1987) 123.
[26] E.D. Wachsman, N. Jiang, C.W. Frank, D.M. Mason, D.A. Stevenson, Appl. Phys. A 50 (1990) 545.
[27] S.E. Paje, J. Llopis, Appl. Phys. A 59 (1994) 569.
[28] Y. Chen, R.T. Williams, W.A. Sibley, Phys. Rev. 182 (1969) 960.
[29] K.H. Lee, J.H. Crawford Jr., Appl. Phys. Lett. 33 (1978) 273.
[30] W.C. Oliver, C.J. McHargue, G.C. Farlow, C.W. White, in: J.H. Crawford Jr., Y. Chen, W.A. Sibley (Eds.), Defect Properties and Processing of High-Technology Nonmetallic Materials, Mater. Res. Soc. Symp. Proc. 24, Pittsburgh, PA, 1984, p. 515.
[31] R.W. Davidge, J. Nucl. Mater. 25 (1968) 75.
[32] W.C. McGowan, W.A. Sibley, Philos. Mag. 19 (1969) 967.